Supplementary files

Confinement of Au^{3+}-Rich Clusters by Silicalite-1 for Selective Solvent-Free Oxidation of Toluene

He Huang,[a,#] Wanyue Ye,[a,#] Caicheng Song,[a] Yingcen Liu,[a] Xiaotong Zhang,[b] Yu Shan,[a] Yuzhen Ge*[,c] and Shufen Zhang,[a] Rongwen Lu*[,a]

[a]State Key Laboratory of Fine Chemicals, Dalian University of Technology, Dalian 116024, Liaoning, PR China

[b]Department of Catalytical Chemistry and Engineering, State Key Laboratory of Fine Chemicals, Dalian University of Technology, Dalian 116024, Liaoning, PR China

[c]Beijing National Laboratory for Molecular Sciences, College of Chemistry and Molecular Engineering, Peking University, Beijing 100871, PR China

Corresponding Author
Rongwen Lu, email: lurw@dlut.edu.cn
Yuzhen Ge, email: gyzhen822@pku.edu.cn

[#]He Huang and Wanyue Ye contributed equally to this work.

Table S1 Au loadings of all Au catalysts.

Sample	Au loading[a] (wt%)
Silicalite-1	--
0.01Au@Silicalite-1	1.06
0.02Au@Silicalite-1	2.12
0.03Au@Silicalite-1	3.19
0.04Au@Silicalite-1	4.25
0.01Au^{3+}@Silicalite-1	1.13
0.02Au^{3+}@Silicalite-1	2.31
0.03Au^{3+}@Silicalite-1	3.45
0.01Au/SiO_2	1.09
0.02Au/SiO_2	2.24
0.03Au/SiO_2	3.31
0.03Au/Silicalite-1	3.38

a: Au loadings were analyzed by inductively coupled plasma atomic emission spectroscopy (ICP-AES).

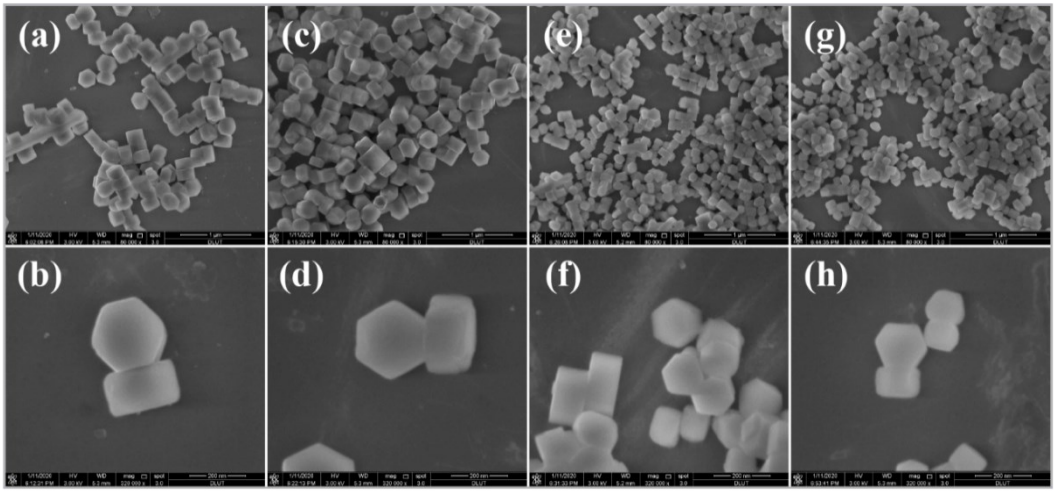

Figure S1 SEM images of 0.01Au@Silicalite-1 (a, b), 0.02Au@Silicalite-1 (c, d), 0.03Au@Silicalite-1 (e, f) and 0.04Au@Silicalite-1 (g, h). Scale bar = 1 μm and 200 nm, respectively.

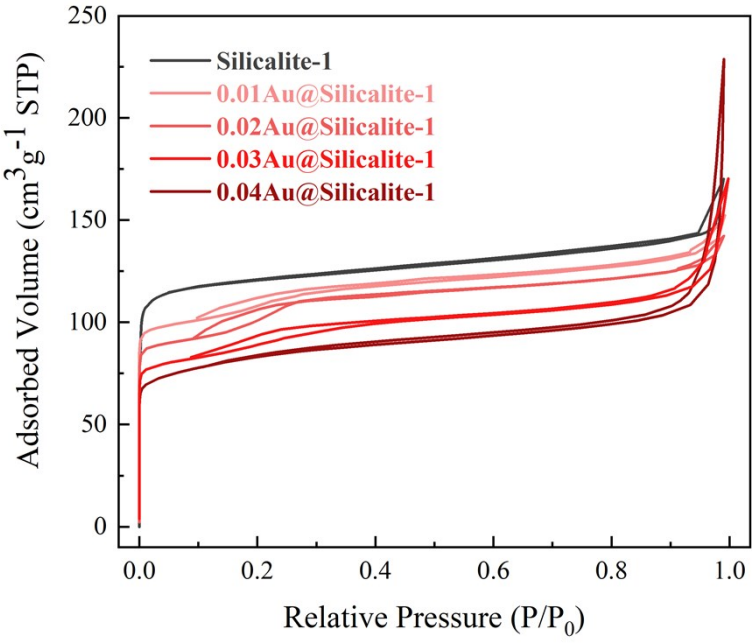

Figure S2 N_2 adsorption/desorption isotherms of Au@Silicalite-1 with different Au loadings.

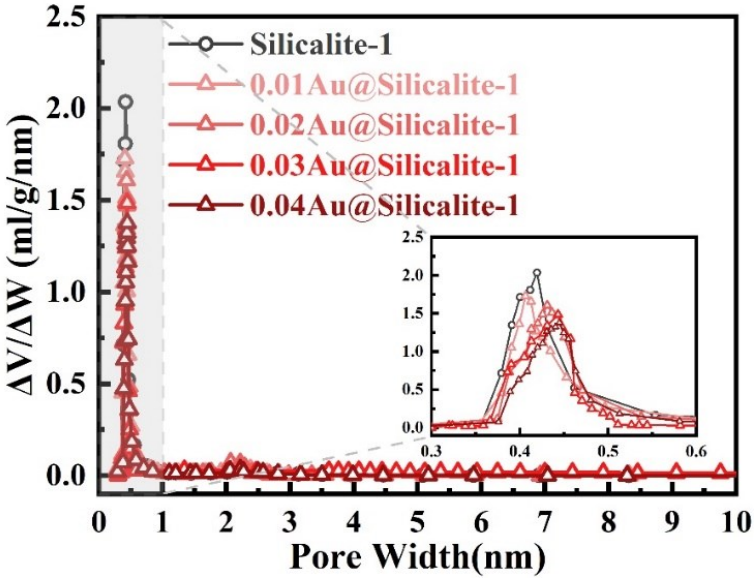

Figure S3 Micropore size distribution of Au@Silicalite-1 with different Au loadings.

Table S2 General characterization results of all Au catalysts.

Sample	d_{TEM}[a] (nm)	S_{BET}[b] (m^2/g)	S_{micro}[c] (m^2/g)	S_{ext}[c] (m^2/g)	V_{micro}[d] (ml/g)
Silicalite-1	--	405	353	52	0.17
0.01Au@Silicalite-1	2.2	385	334	51	0.16
0.02Au@Silicalite-1	3.3	368	336	32	0.15
0.03Au@Silicalite-1	4.5	335	290	45	0.15
0.04Au@Silicalite-1	5.8	316	272	44	0.13
0.03Au/SiO_2	27.5	324	71	253	0.13
0.03Au/Silicalite-1	27.3	360	273	87	0.12

a: The diameter of Au clusters (d_{TEM}) was estimated from TEM analysis. $d_{TEM} = \Sigma n_i d_i^3 / \Sigma n_i d_i^2$, where n_i is the number of crystallites with a diameter d_i.

b: S_{BET} (surface area) was calculated by applying the BET equation using the linear part ($0.01 < P/P_0 < 0.15$) of the adsorption isotherm.

c: S_{micro} (micropore area) and S_{ext} (external surface area) were calculated using the *T-plot* method.

d: V_{micro} (micropore volume) was calculated using the *T-plot* method.

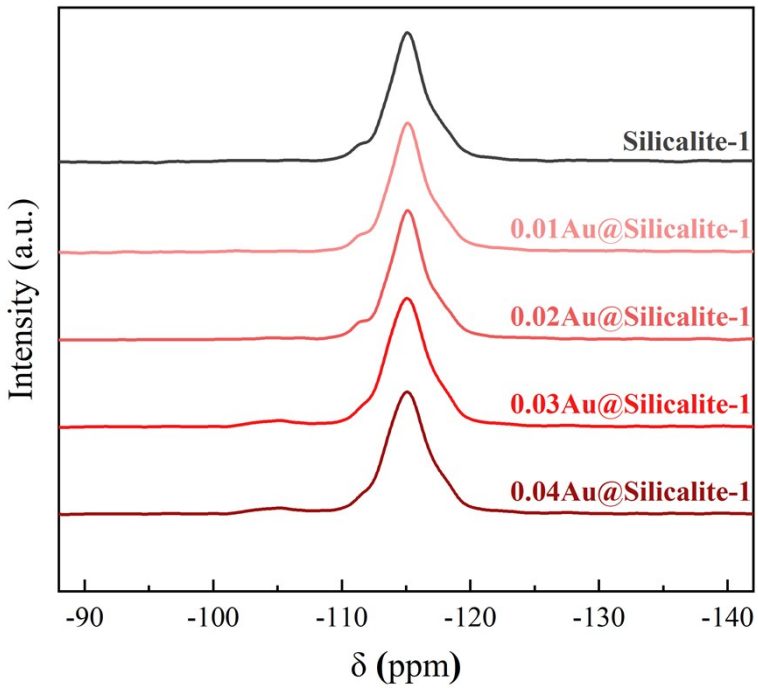

Figure S4 ^{29}Si NMR spectra of samples with different Au loadings.

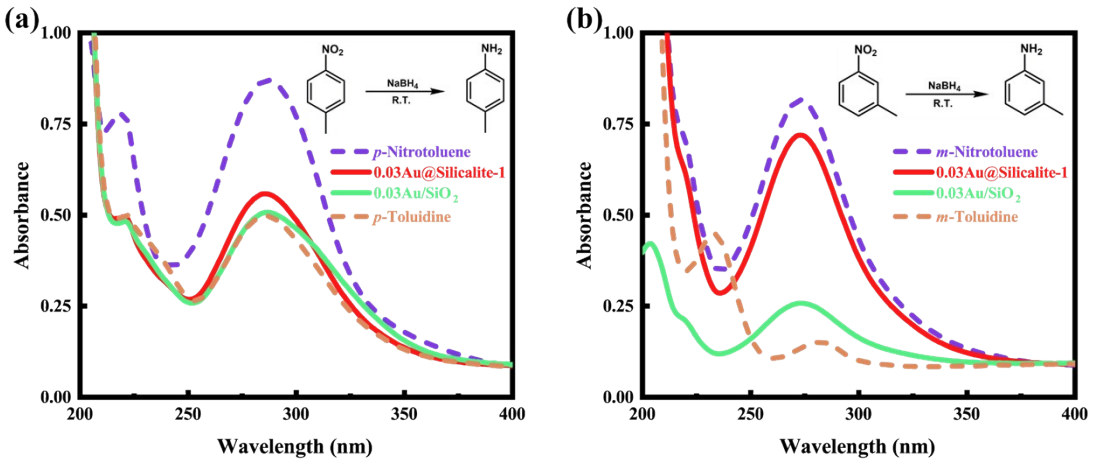

Figure S5 UV-vis absorption spectra of 0.03Au@Silicalite-1 and 0.03Au/SiO_2 catalysts in the reduction of *p*-nitrotoluene (a) and *m*-nitrotoluene (b) compared with the corresponding standard substance.

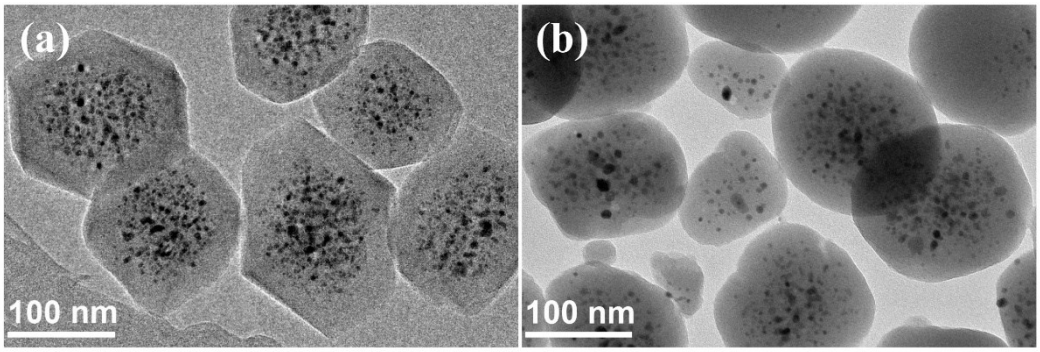

Figure S6 TEM images of 0.03Au@Silicalite-1 before (a) and after (b) long-term grinding.

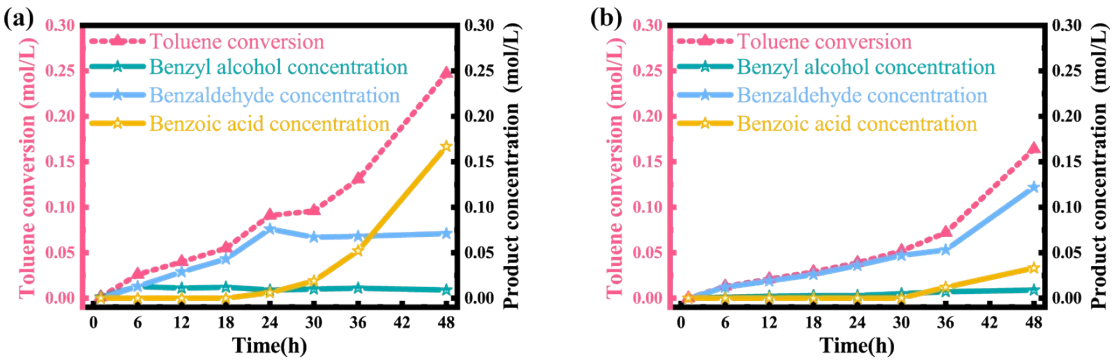

Figure S7 Controlled experiments for toluene oxidation: (a) reaction without catalyst, (b) reaction with pure Silicalite-1 as catalyst. Reaction conditions: 160 °C (433 K), 9.2 g (0.1 mol) toluene, 1 MPa O_2, and 0.1 g Silicalite-1 for (b).

Table S3 Catalytic performance comparison of different catalysts recently reported in the solvent-free liquid-phase oxidation of toluene by oxygen to benzaldehyde.

Catalyst	Toluene conversion (%)	Benzaldehyde selectivity (%)	Benzaldehyde yield (%)	Substrate /catalyst mass ratio	TON	Ref
Pd/Bi_2WO_6	3.4	90.0	3.1	24	14.4	[1]
8-CN-600	2.0	99.0	2.0	115	30.1	[2]
$CuFe/\gamma\text{-}Al_2O_3$	7.3	86.0	6.3	43	55.8	[3]
F-0.5-PACN	1.0	96.0	1.0	24	58.7	[4]
Co(II)TPP/CTS	8.8	37.0	3.3	81	69.8	[5]
Mg_3Al-LDH	8.7	97.5	8.5	51	78.7	[6]
MnO_x/SBA-15	15.9	37.6	6.0	216	120.0	[7]
Pd-PMHS/TiO_2	1.6	56.1	0.9	92	130.0	[8]
Co@N/Co-CNT	28.0	9.8	2.7	45	224.5	[9]
0.03Au/Silicalite-1	**10.7**	**90.5**	**9.7**	**2884**	**660.7**	**This work**
0.03Au/Silicalite-1	**19.9**	**90.1**	**18.0**	**1442**	**614.4**	**This work**

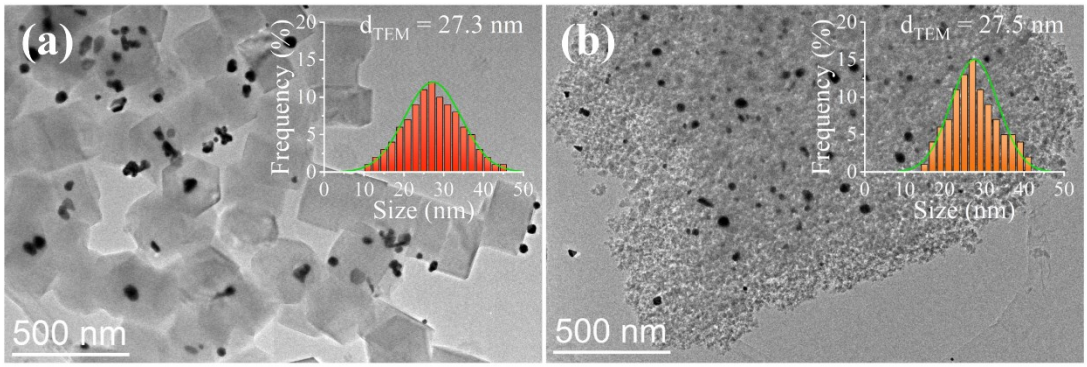

Figure S8 TEM images of 0.03Au/Silicalite-1 (a) and 0.03Au/SiO_2 (b) and the corresponding size distribution of Au nanoparticles. Scale bar = 500 nm.

Table S4 Solvent-free catalytic oxidation of toluene at different reaction time.

Catalyst	Time (h)	Conversion (%)	Selectivity (%)			Carbon balance (γ) / %	TON	TOF
			Benzyl alcohol	Benzal-dehyde	Benzoic acid			
0.01Au@Silicalite-1	12	1.3	6.1	93.4	0.5	99.7	241.6	20.1
0.01Au@Silicalite-1	24	2.6	6.2	92.5	1.3	98.8	483.1	20.1
0.01Au@Silicalite-1	36	3.2	4.6	83.3	12.1	98.1	594.6	16.5
0.01Au@Silicalite-1	48	3.9	4.4	74.2	21.4	97.9	724.7	15.1
0.02Au@Silicalite-1	12	3.1	6.7	92.7	0.6	98.0	288.0	24.0
0.02Au@Silicalite-1	24	5.9	6.8	91.7	1.5	97.6	548.2	22.8
0.02Au@Silicalite-1	36	7.5	5.4	80.9	13.7	97.1	696.8	19.4
0.02Au@Silicalite-1	48	8.8	5.6	68.7	25.7	96.9	817.6	17.0
0.03Au@Silicalite-1	12	5.9	5.8	91.7	2.5	97.4	364.3	30.4
0.03Au@Silicalite-1	24	10.7	5.7	90.5	3.8	96.4	660.7	27.5
0.03Au@Silicalite-1	36	13.4	4.6	74.8	20.6	93.7	827.4	23.0
0.03Au@Silicalite-1	48	16.3	4.2	69.5	26.3	91.3	1006.5	21.0
0.04Au@Silicalite-1	12	4.1	5.9	89.7	4.4	97.8	190.0	15.8
0.04Au@Silicalite-1	24	6.9	5.4	83.2	11.4	98.5	319.8	13.3
0.04Au@Silicalite-1	36	7.8	4.9	79.7	15.4	97.2	361.5	10.0
0.04Au@Silicalite-1	48	8.6	4.7	76.5	18.8	96.8	398.6	8.3

Reaction conditions: 160 °C (433 K), 1 MPa O_2, 9.2 g toluene, 0.1 g catalyst, stirring rate of 1500 rpm.

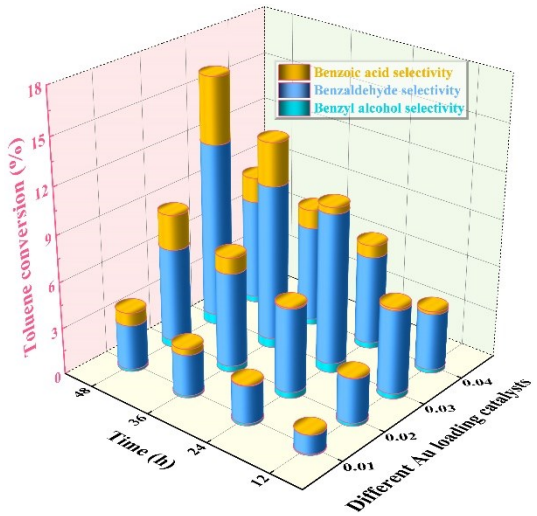

Figure S9 Solvent-free catalytic oxidation of toluene at different reaction time.

The conversion of toluene increased with the prolonged reaction time despite the various loadings of Au in Au@Silicalite-1. However, the over oxidation of benzaldehyde to benzoic acid increased with the extended reaction time. Considering both the conversion of toluene and selectivity of benzaldehyde, the reaction time of 24 h was chose as the optimized condition.

Table S5 Solvent-free catalytic oxidation of toluene at different reaction temperatures.

Catalyst	Temperature (℃)	Conversion (%)	Selectivity (%)			Carbon balance (γ) / %	TON	TOF
			Benzyl alcohol	Benzal-dehyde	Benzoic acid			
0.01Au@Silicalite-1	140	0.2	0.5	99.5	0	100.0	37.2	1.5
0.01Au@Silicalite-1	160	2.6	6.2	92.5	1.3	98.8	483.1	20.1
0.01Au@Silicalite-1	180	6.1	1.4	40.3	58.3	97.5	1133.5	47.2
0.02Au@Silicalite-1	140	0.3	0.6	99.4	0	100.0	27.9	1.2
0.02Au@Silicalite-1	160	5.9	6.8	91.7	1.5	97.6	548.2	22.8
0.02Au@Silicalite-1	180	13.8	1.1	41.2	57.7	93.5	1282.2	53.4
0.03Au@Silicalite-1	140	0.3	0.6	99.4	0	100.0	18.5	0.8
0.03Au@Silicalite-1	160	10.7	5.7	90.5	3.8	96.4	660.7	27.5
0.03Au@Silicalite-1	180	21.9	1.2	47.3	51.5	90.9	1352.2	56.3
0.04Au@Silicalite-1	140	0.2	0.7	99.3	0	100.0	9.3	0.4
0.04Au@Silicalite-1	160	6.9	5.4	83.2	11.4	98.5	319.8	13.3
0.04Au@Silicalite-1	180	15.6	0.7	39.9	59.4	93.1	723.0	30.1

Reaction conditions: 24 h, 1 MPa O_2, 9.2 g toluene, 0.1 g catalyst, stirring rate of 1500 rpm.

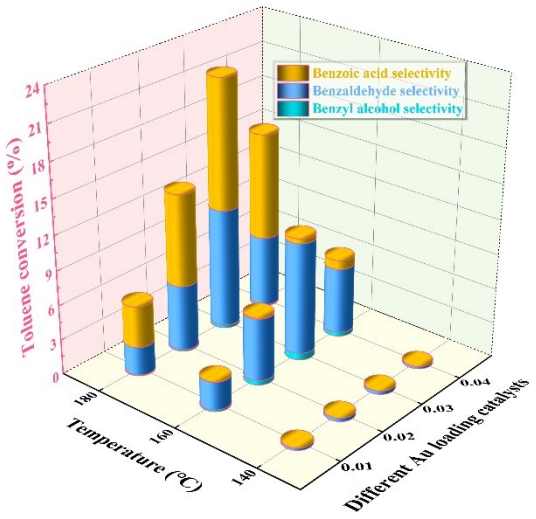

Figure S10 Solvent-free catalytic oxidation of toluene at different reaction temperatures.

The conversion of toluene markedly promoted with the increased reaction temperatures despite the various loadings of Au in Au@Silicalite-1. However, the severely over oxidation of benzaldehyde to benzoic acid happened the same time. Considering both the conversion of toluene and selectivity of benzaldehyde, the reaction temperature of 160 ℃ was chose as the optimized condition.

Table S6 Solvent-free catalytic oxidation of toluene at different O_2 pressure.

Catalyst	O_2 pressure (MPa)	Conversion (%)	Selectivity (%)			Carbon balance (γ) / %	TON	TOF
			Benzyl alcohol	Benzal-dehyde	Benzoic acid			
0.01Au@Silicalite-1	0.5	1.2	6.9	92.8	0.3	99.7	223.0	9.3
0.01Au@Silicalite-1	1.0	2.6	6.2	92.5	1.3	98.8	483.1	20.1
0.01Au@Silicalite-1	1.5	2.9	5.7	91.1	3.2	98.7	538.9	22.5
0.02Au@Silicalite-1	0.5	2.8	7.1	92.1	0.8	98.7	260.1	10.8
0.02Au@Silicalite-1	1.0	5.9	6.8	91.7	1.5	97.6	548.2	22.8
0.02Au@Silicalite-1	1.5	6.5	6.1	90.1	3.8	97.4	603.9	25.2
0.03Au@Silicalite-1	0.5	5.2	6.6	91.4	2	97.8	321.1	13.4
0.03Au@Silicalite-1	1.0	10.7	5.7	90.5	3.8	96.4	660.7	27.5
0.03Au@Silicalite-1	1.5	11.9	5.2	89.1	5.7	96.2	734.8	30.6
0.04Au@Silicalite-1	0.5	3.3	6.2	89.5	4.3	98.4	152.9	6.4
0.04Au@Silicalite-1	1.0	6.9	5.4	83.2	11.4	98.5	319.8	13.3
0.04Au@Silicalite-1	1.5	7.4	5	81.7	13.3	97.6	343.0	14.3

Reaction conditions: 160 °C (433 K), 24 h, 9.2 g toluene, 0.1 g catalyst, stirring rate of 1500 rpm.

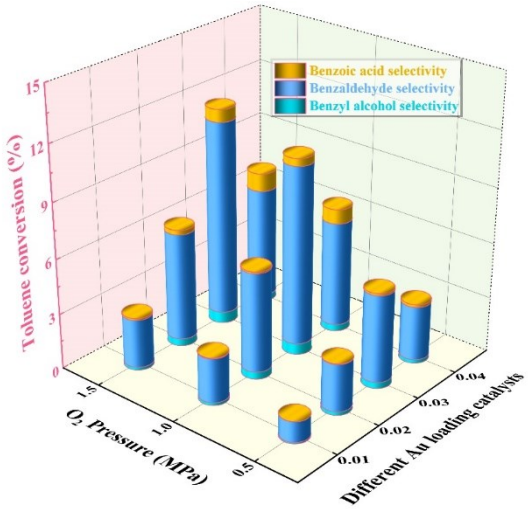

Figure S11 Solvent-free catalytic oxidation of toluene at different O_2 pressure.

The conversion of toluene increased with the increasing pressure of O_2, especially at low pressures. However, the selectivity of products was slightly influenced by the changing of O_2 pressure.

Table S7 Solvent-free catalytic oxidation of toluene with different dose of catalyst.

Catalyst	Dose of catalyst (g)	Conversion (%)	Selectivity (%)			Carbon balance (γ) / %	TON	TOF
			Benzyl alcohol	Benzal-dehyde	Benzoic acid			
0.01Au@Silicalite-1	0.05	1.1	5.9	92.9	1.2	99.8	408.8	17.0
0.01Au@Silicalite-1	0.1	2.6	6.2	92.5	1.3	98.8	483.1	20.1
0.01Au@Silicalite-1	0.2	5.0	5.9	92.2	1.9	97.8	464.6	19.4
0.02Au@Silicalite-1	0.05	2.9	6.2	92.3	1.5	98.7	538.9	22.5
0.02Au@Silicalite-1	0.1	5.9	6.8	91.7	1.5	97.6	548.2	22.8
0.02Au@Silicalite-1	0.2	11.6	6.5	91.3	2.2	96.3	538.9	22.5
0.03Au@Silicalite-1	0.05	5.4	6.1	91.1	2.8	97.9	669.0	27.9
0.03Au@Silicalite-1	0.1	10.7	5.7	90.5	3.8	96.4	660.7	27.5
0.03Au@Silicalite-1	0.2	19.9	5.6	90.1	4.3	90.7	614.4	25.6
0.04Au@Silicalite-1	0.05	3.4	5.9	84.1	10	98.5	315.9	13.2
0.04Au@Silicalite-1	0.1	6.9	5.4	83.2	11.4	98.5	319.8	13.3
0.04Au@Silicalite-1	0.2	13.7	5.1	82.8	12.1	96.0	317.5	13.2

Reaction conditions: 160 °C (433 K), 24 h, 1 MPa O_2, 9.2 g toluene, stirring rate of 1500 rpm.

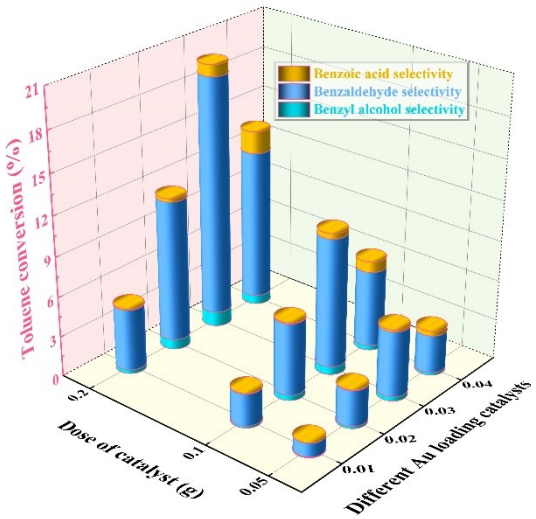

Figure S12 Solvent-free catalytic oxidation of toluene with different dose of catalyst.

The conversion of toluene linearly increased with the increasing dosing amount of catalysts. However, the selectivity of products was slightly influenced by the amount of catalysts.

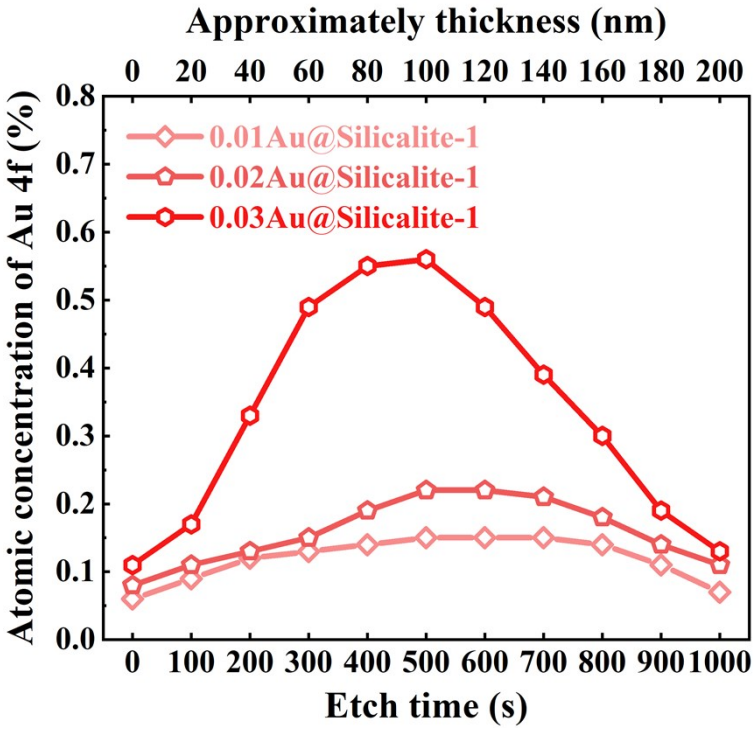

Figure S13 Etching time or deepness dependent Au content curves by destructive elemental depth profiles of XPS measurement for 0.01Au@Silicalite-1, 0.02Au@Silicalite-1 and 0.03Au@Silicalite-1.

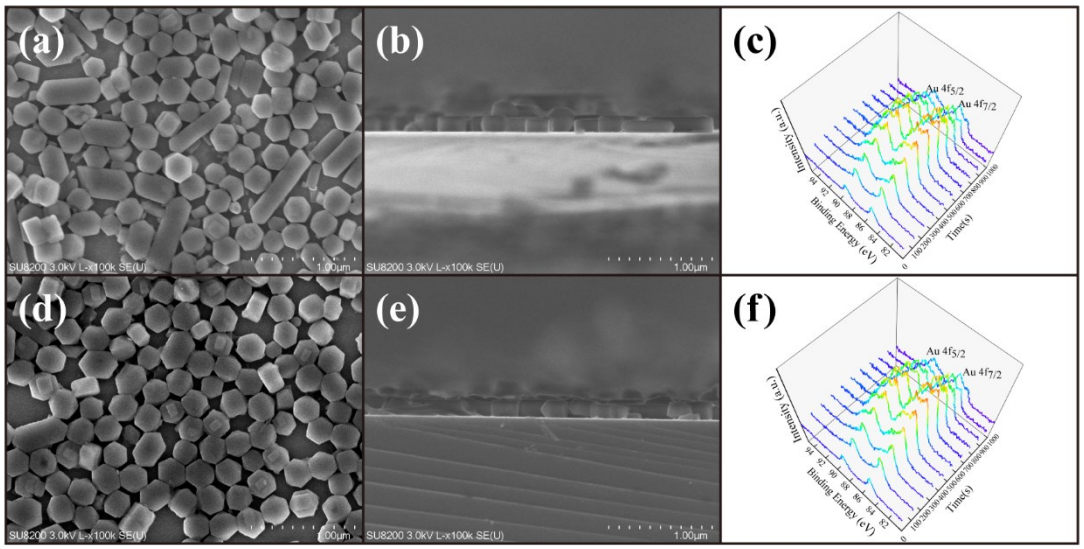

Figure S14 Destructive elemental depth profiles of 0.01Au@Silicalite-1 by XPS measurements. (a) SEM planar graph, (b) SEM sectional graph, (c) XPS high-resolution spectra of Au 4f. Destructive elemental depth profiles of 0.02Au@Silicalite-1 by XPS measurements. (d) SEM planar graph, (e) SEM sectional graph, (f) XPS high-resolution spectra of Au 4f.

Table S8 The concentration of atomic Au 4f and the proportion of Au^{3+} and Au^{0} in every layer of samples.

Sample layer	Etch time (s)	A_{Au4f}%[a]	P_{Au3+}%[b]	P_{Au0}%[b]
0.01Au@Silicalite-1 layer0	0	0.06	0%	100%
0.01Au@Silicalite-1 layer1	100	0.09	41%	59%
0.01Au@Silicalite-1 layer2	200	0.12	48%	52%
0.01Au@Silicalite-1 layer3	300	0.13	53%	47%
0.01Au@Silicalite-1 layer4	400	0.14	66%	34%
0.01Au@Silicalite-1 layer5	500	0.15	82%	18%
0.02Au@Silicalite-1 layer0	0	0.08	0%	100%
0.02Au@Silicalite-1 layer1	100	0.11	48%	52%
0.02Au@Silicalite-1 layer2	200	0.13	49%	51%
0.02Au@Silicalite-1 layer3	300	0.15	60%	40%
0.02Au@Silicalite-1 layer4	400	0.19	70%	30%
0.02Au@Silicalite-1 layer5	500	0.22	83%	17%
0.03Au@Silicalite-1 layer0	0	0.11	0%	100%
0.03Au@Silicalite-1 layer1	100	0.17	57%	43%
0.03Au@Silicalite-1 layer2	200	0.33	64%	36%
0.03Au@Silicalite-1 layer3	300	0.49	78%	22%
0.03Au@Silicalite-1 layer4	400	0.55	80%	20%
0.03Au@Silicalite-1 layer5	500	0.56	84%	16%
0.03Au/Silicalite-1 surface layer	--	0.70	0%	100%
0.03Au/SiO_2 surface layer	--	0.75	0%	100%

a: A_{Au4f}% is atomic concentration of Au 4f calculated by the relative correction factor of the test instrument.

b: $P_{Au^{3+}}$% and $P_{Au^{0}}$% are the proportion of Au^{3+} and Au^{0} in every etch layer, and the peaks of the spectra are splited by the software XPS PEAK41.

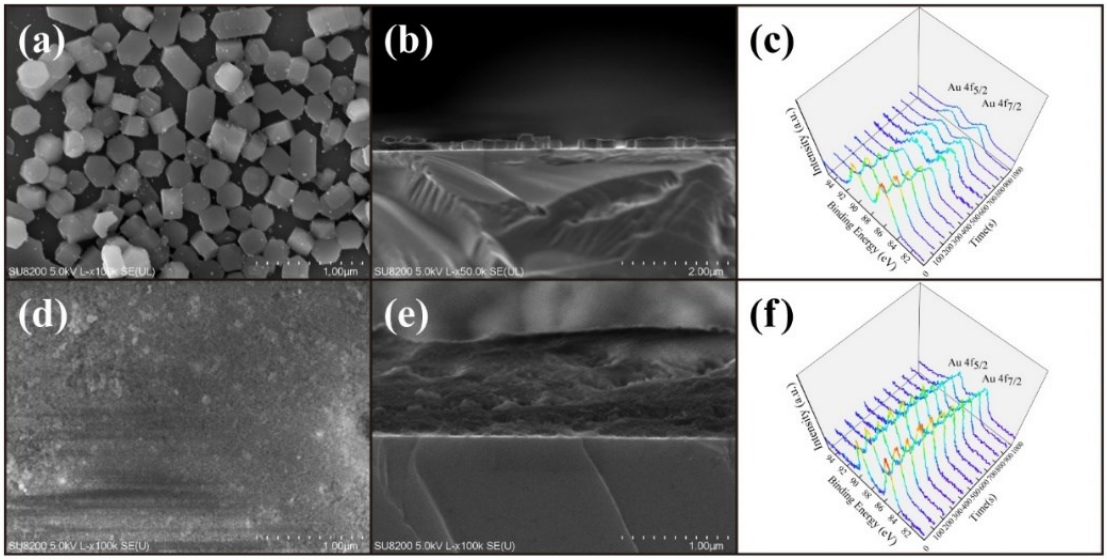

Figure S15 Destructive elemental depth profiles of 0.03Au/Silicalite-1 by XPS measurements (a) SEM planar graph, (b) SEM sectional graph, (c) XPS high-resolution spectra of Au 4f. Destructive elemental depth profiles of 0.03Au/SiO_2 by XPS measurements (d) SEM planar graph, (e) SEM sectional graph, (f) XPS high-resolution spectra of Au 4f.

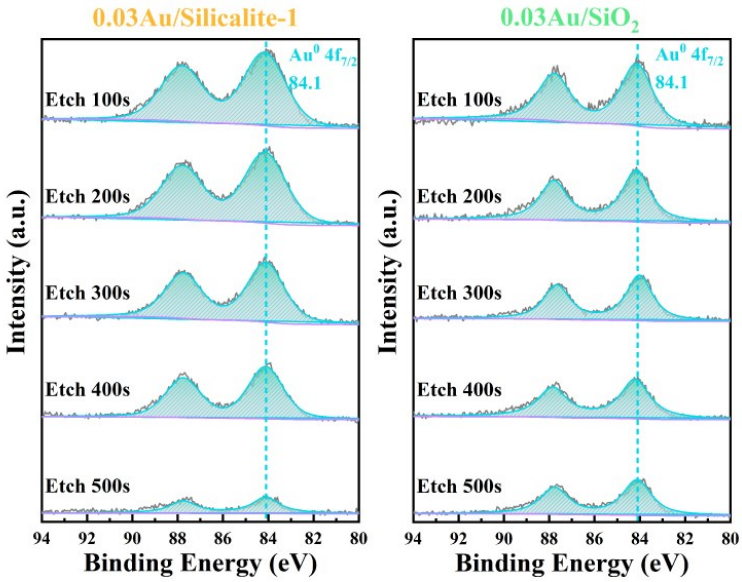

Figure S16 Etching time dependent XPS high-resolution spectra of Au 4f for 0.03Au/Silicalite-1 and 0.03Au/SiO_2.

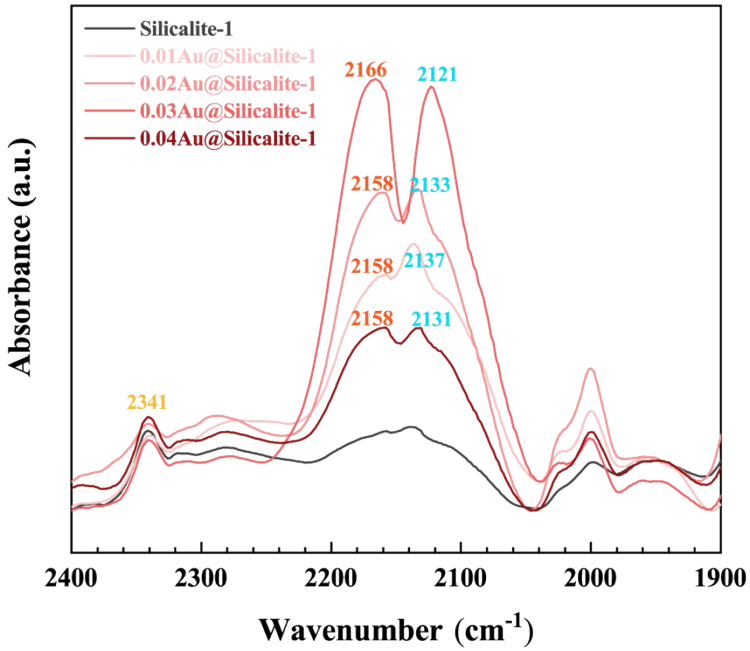

Figure S17 DB-FTIR spectra of in-situ static chemical adsorption of CO for Au@Silicalite-1 samples.

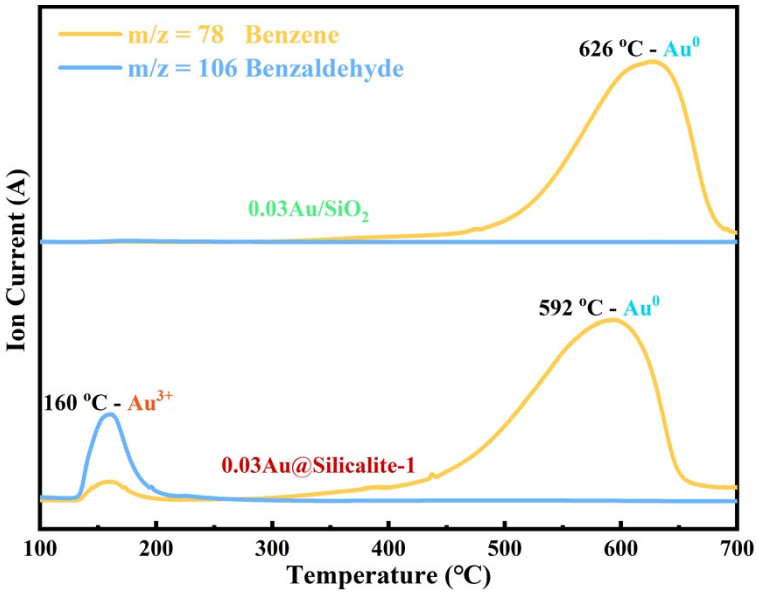

Figure S18 Benzaldehyde TPD profiles of $0.03Au/SiO_2$ and 0.03Au@Silicalite-1.

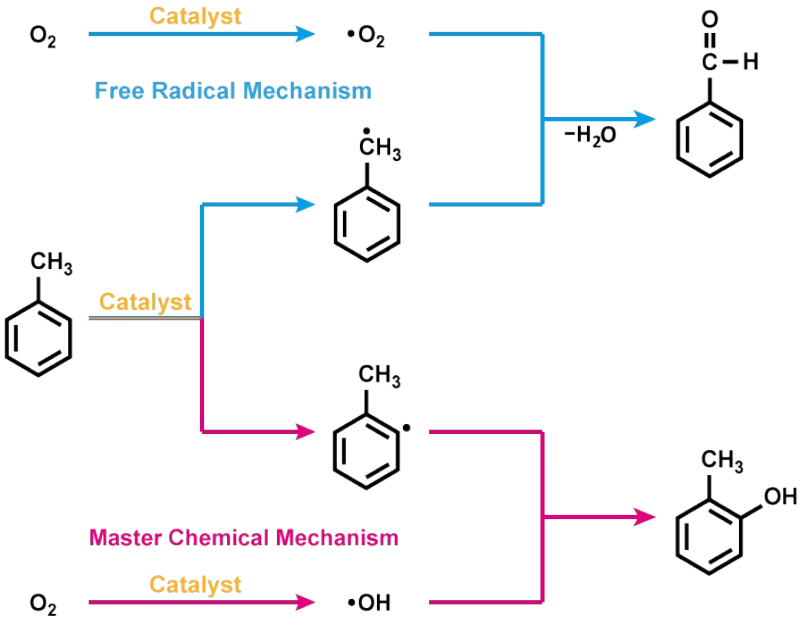

Figure S19 The earlier reported mechanism in literatures for the catalytic oxidation of toluene.[10-13]

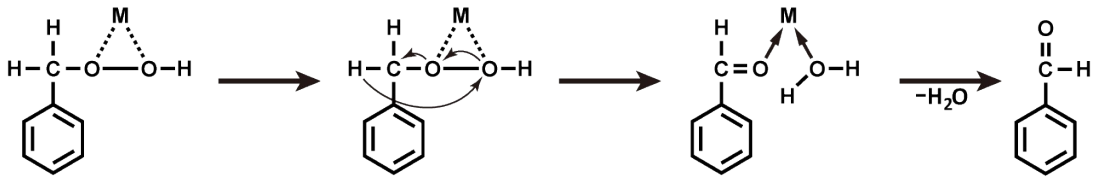

Figure S20 Electron transfer pathway of the intermediate for benzaldehyde production from toluene oxidation.[14]

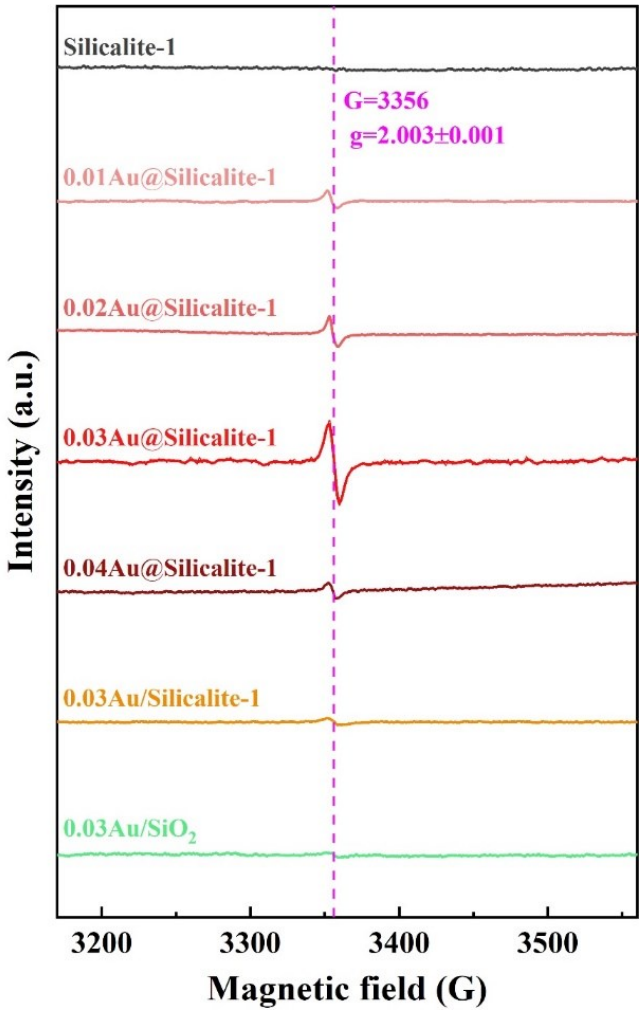

Figure S21 EPR spectra of catalysts at ambient temperature and pressure.

Table S9 Solvent-free catalytic oxidation of toluene with different single active center catalysts.

Catalyst[a]	Conversion (%)	Selectivity (%)			Carbon balance (γ) / %	TON	TOF
		Benzyl alcohol	Benzal-dehyde	Benzoic acid			
0.01Au/SiO_2	2.1	0.7	56.4	42.9	99.1	379.5	15.8
0.01Au^{3+}@Silicalite-1	7.1	5.6	93.8	0.6	97.5	1237.6	51.6
0.02Au/SiO_2	2.8	0.2	36.7	63.1	98.7	246.2	10.3
0.02Au^{3+}@Silicalite-1	17.5	5.1	92.8	2.1	91.1	1492.2	62.2
0.03Au/SiO_2	3.1	0.5	21.8	77.7	98.5	184.5	7.7
0.03Au^{3+}@Silicalite-1	30.3	4.1	92.5	3.4	85.7	1729.9	72.1
0.03Au^{3+}@Silicalite-1[b]	9.6	4.7	91.4	3.9	96.7	548.1	22.8
0.03Au^{3+}@Silicalite-1[c]	2.9	4.4	90.3	5.3	98.6	165.6	6.9

a: Reaction conditions: 160 °C (433 K), 24 h, 1 MPa O_2, 9.2 g (0.1 mol) toluene, 0.1 g catalyst, stirring rate of 1500 rpm.

b: The catalyst Au^{3+}@Silicalite-1 was used in the second time of recycling.
c: The catalyst Au^{3+}@Silicalite-1 was used in the third time of recycling.

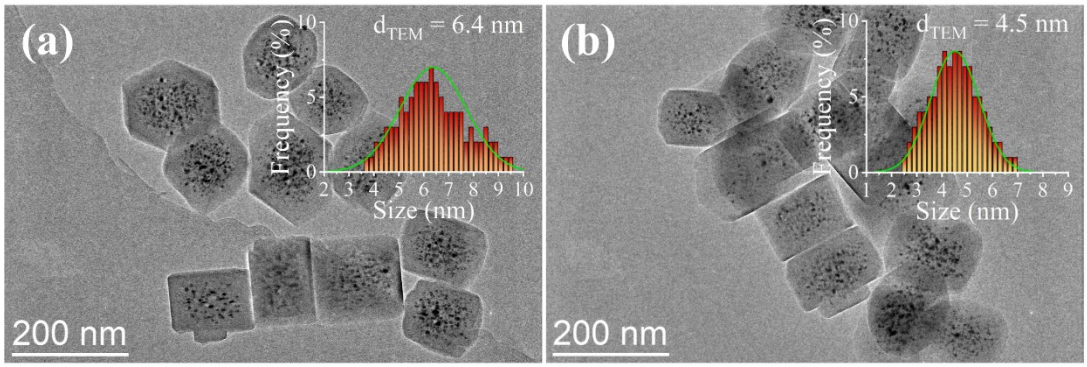

Figure S22 HRTEM images of 0.03Au@Silicalite-1 and size distribution histograms of Au nanoparticles after 10 cycles of stability test for catalytic oxidation of toluene (a), and then after regeneration (b). The average cluster diameter $d_{TEM} = \sum n_i d_i^3 / \sum n_i d_i^2$, where n_i is the number of crystallites having diameter d_i.

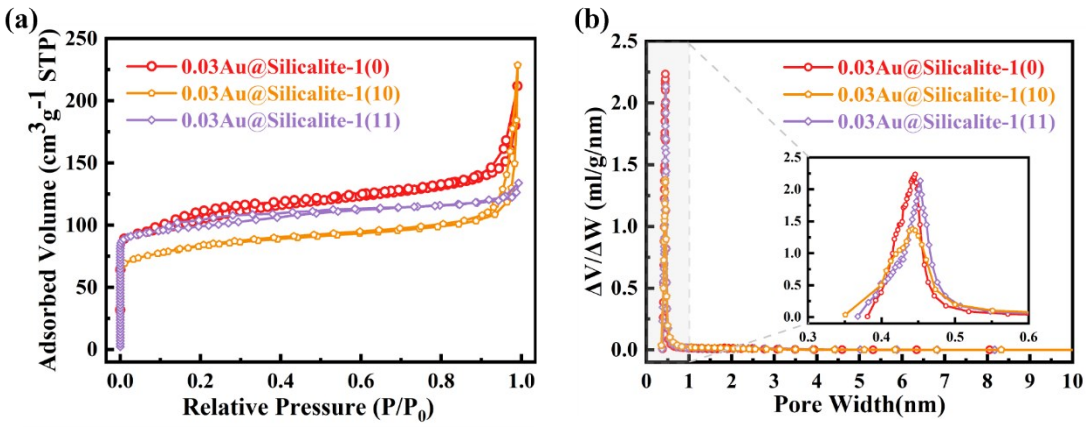

Figure S23 (a) N_2 adsorption/desorption isotherms and (b) micropore size distribution of 0.03Au@Silicalite-1 in unused status and after 10^{th} cycles of stability testing and after regeneration for 11^{th}.

Table S10 Average sizes of Au and porosity of 0.03Au@Silicalite-1 before and after regeneration.

Sample	d_{TEM} (nm)	S_{BET} (m^2/g)	S_{micro} (m^2/g)	S_{ext} (m^2/g)	V_{micro} (ml/g)	V_{total}[a] (ml/g)	D_{pore}[b] (nm)
0.03Au@Silicalite-1(0)	4.5	335	290	45	0.15	0.33	0.47
0.03Au@Silicalite-1(10)	6.4	301	179	122	0.08	0.25	0.58
0.03Au@Silicalite-1(11)	4.5	330	263	67	0.12	0.31	0.51

a： V_{total} (total pore volume) was calculated by $P/P_0 = 0.99$ and hole diameter < 200 nm.

b： D_{pore} (average pore diameter) was calculated using the *H-K(Original)* method.

References

1. B. Yuan, B. Zhang, Z. Wang, S. Lu, J. Li, Y. Liu and C. Li, *Chin. J. Catal.*, 2017, **38**, 440-446.
2. X. Wang and Y. Li, *J. Mater. Chem. A*, 2016, **4**, 5247-5257.
3. F. Wang, J. Xu, X. Li, J. Gao, L. Zhou and R. Ohnishi, *Adv. Synth. Catal.*, 2005, **347**, 1987-1992.
4. L. Jing, D. Wang, M. He, Y. Xu, M. Xie, Y. Song, H. Xu and H. Li, *J. Hazard. Mater.*, 2021, **401**, 123309.
5. G. Huang, A. P. Wang, S. Y. Liu, Y. A. Guo, H. Zhou and S. K. Zhao, *Catal. Lett.*, 2007, **114**, 174-177.
6. X. Wang, G. Wu, H. Liu and Q. Lin, *Catalysts*, 2016, **6**, 14.
7. W. Zhong, S. R. Kirk, D. Yin, Y. Li, R. Zou, L. Mao and G. Zou, *Chem. Eng. J.* , 2015, **280**, 737-747.
8. B. Fu, X. Zhu and G. Xiao, *Appl. Catal., A*, 2012, **415-416**, 47-52.
9. B. Chen, S. Li, S. Liu, M. Dong, B. Han, H. Liu and L. Zheng, *J. Mater. Chem. A*, 2019, **7**, 27212-27216.
10. K. T. V. Rao, P. S. N. Rao, P. Nagaraju, P. S. S. Prasad and N. Lingaiah, *J. Mol. Catal. A: Chem.*, 2009, **303**, 84-89.
11. N. I. Kuznetsova, N. V. Kirillova, L. I. Kuznetsova, M. Y. Smirnova and V. A. Likholobov, *J. Hazard. Mater.*, 2007, **146**, 569-576.
12. K. Nomiya, K. Hashino, Y. Nemoto and M. Watanabe, *J. Mol. Catal. A: Chem.*, 2001, **176**, 79-86.
13. R. Neumann and M. de la Vega, *J. Mol. Catal.*, 1993, **84**, 93-108.
14. W. Partenheimer, *J. Mol. Catal. A: Chem.*, 2003, **206**, 105-119.